

Phase-modulated dynamical decoupling sequences robust to systematic amplitude error

Sijie Chen(陈思婕), Guanxing Chen(陈官幸), Jiahao Huang(黄嘉豪), Peiliang Liu(刘培亮), Min Zhuang(庄敏), and Chaohong Lee(李朝红)

Citation: Chin. Phys. B, 2025, 34 (**7**): 074202. DOI: 10.1088/1674-1056/adcd43
http://cpb.iphy.ac.cn; http://iopscience.iop.org/cpb

What follows is a list of articles you may be interested in

A novel dual-channel thermo-optic locking method for the whispering gallery mode microresonator

Wenjie Fan(范文杰), Wenyao Liu(刘文耀), Ziwen Pan(潘梓文), Rong Wang(王蓉), Lai Liu(刘来), Enbo Xing(邢恩博), Yanru Zhou(周彦汝), Jun Tang(唐军), and Jun Liu(刘俊)
Chin. Phys. B, 2024, 33 (**5**): 054206. DOI: 10.1088/1674-1056/ad225f

Calibration of quantitative rescattering model for simulating vortex high-order harmonic generation driven by Laguerre-Gaussian beam with nonzero orbital angular momentum

Jiaxin Han(韩嘉鑫), Zhong Guan(管仲), Beiyu Wang(汪倍羽), and Cheng Jin(金成)
Chin. Phys. B, 2023, 32 (**12**): 124210. DOI: 10.1088/1674-1056/acfa86

Tailoring OAM spectrum of high-order harmonic generation driven by two mixed Laguerre-Gaussian beams with nonzero radial nodes

Beiyu Wang(汪倍羽), Jiaxin Han(韩嘉鑫), and Cheng Jin(金成)
Chin. Phys. B, 2023, 32 (**12**): 124208. DOI: 10.1088/1674-1056/ad0144

Enhanced phase sensitive amplification towards improving noise immunity

Hui Guo(郭辉), Zhi Li(李治), Hengxin Sun(孙恒信), Kui Liu(刘奎), and Jiangrui Gao(郜江瑞)
Chin. Phys. B, 2023, 32 (**5**): 054204. DOI: 10.1088/1674-1056/acbdeb

Tunable phonon-atom interaction in a hybrid optomechanical system

Yao Li(李耀), Chuang Li(李闯), Jiandong Zhang(张建东), Ying Dong(董莹), and Huizhu Hu(胡慧珠)
Chin. Phys. B, 2023, 32 (**4**): 044213. DOI: 10.1088/1674-1056/acb9ea

---

Phase-modulated dynamical decoupling sequences robust to systematic amplitude error

Sijie Chen(陈思婕)[1,2,†], Guanxing Chen(陈官幸)[1,†], Jiahao Huang(黄嘉豪)[1], Peiliang Liu(刘培亮)[1,‡], Min Zhuang(庄敏)[2,§], and Chaohong Lee(李朝红)[2]

[1] *Laboratory of Quantum Engineering and Quantum Metrology & School of Physics and Astronomy, Sun Yat-Sen University (Zhuhai Campus), Zhuhai* 519082, *China*

[2] *Institute of Quantum Precision Measurement, State Key Laboratory of Radio Frequency Heterogeneous Integration, College of Physics and Optoelectronic Engineering, Shenzhen University, Shenzhen* 518060, *China*

(Received 17 February 2025; revised manuscript received 14 April 2025; accepted manuscript online 16 April 2025)

Dynamical decoupling (DD), usually implemented by sophisticated sequences of instantaneous control pulses, is a well-established quantum control technique for quantum information and quantum sensing. In practice, the pulses are inevitably imperfect with many systematic errors that may influence the performances of DD. In particular, Rabi error and detuning are primary systemic errors arising from finite pulse duration, incorrect time control, and frequency instability. Here, we propose a phase-modulated DD with staggered global phases for the basic units of the pulse sequences to suppress these systemic errors. By varying the global phases appended to the pulses in the dynamical decoupling unit alternatively with 0 or π, our protocol can significantly reduce the influences of Rabi error and detuning. Our protocol is general and can be combined with the most existing DD sequences such as universal DD, knill DD, XY, etc. As an example, we further apply our method to quantum lock-in detection for measuring time-dependent alternating signals. Our study paves the way for a simple and feasible way to realize robust dynamical decoupling sequences, which can be applicable for various quantum sensing scenarios.

Keywords: dynamical decoupling, quantum sensing, quantum lock-in amplifier

PACS: 42.50.Dv, 03.67.–a, 03.65.Ta

DOI: 10.1088/1674-1056/adcd43 **CSTR:** 32038.14.CPB.adcd43

1. Introduction

Dynamical decoupling (DD) is a well-established quantum control technique and widely used in a wide range of applications,[1–8] such as protecting qubits from decoherence,[9–14] increasing the signal-to-noise ratio of quantum sensors for alternating signals,[15] implementing high-fidelity quantum gates,[16] and detecting noise spectrum.[17] In general, a DD sequence is based on the ideas that underlie the spin-echo effect and comprised a series of pulses, separated by certain interpulse delays.[18] In experiments, there are many systematic errors that may influence DD sequence, especially for a larger number of pulses.[19–21] For example, the incorrect time duration or laser strength is called Rabi error[22] which cause the rotation angle error. Moreover, the incorrect laser frequency leads to the detuning.[23] These errors can cause DD scheme fail to achieve the expected performance. To suppress these imperfections, different DD sequences have been proposed, such as XY(4,8,16,...),[23] knill-dynamical-decoupling (KDD),[24,25] and universal dynamical decoupling (UDD) sequences[26] and so on.[47] Especially, a phase randomization protocol for DD sequences has been proposed and realized in experiment to efficiently suppress spurious response, while maintaining the expected signal.[13,27] However, these protocols are not absolutely robust against to the undesired effects as mentioned above. Hence, how to develop a universal DD method with high robustness against systematic errors remains a challenging task.

Meanwhile, it is well known that DD methods has been extensively used to realize the quantum lock-in detection for quantum sensing, such as frequency measurement,[28–30] magnetic field sensing,[28,31] vector light shift detection,[32] and weak-force detection.[33] However, these systemic errors may also influence the quantum lock-in detection. Therefore, it is important to improve the DD sequences for realizing a quantum lock-in detection with high robustness against these errors.

Based on the existing study, it is natural to ask the following questions: (i) Can one develop a universal DD method with robustness against the systematic errors? (ii) Can one realize a robust quantum lock-in detection with this method? In this work, we propose a robust phase-modulated dynamical decoupling sequence to suppress the Rabi error and detuning. Our protocol adds the global phases Φ_m which are 0 or π alternately to all the pulses of each unit. This pro-

[†]These authors contributed equally to this work.

[‡]Corresponding author. E-mail: liupliang@mail.sysu.edu.cn

[§]Corresponding author. E-mail: mmzhuang@szu.edu.cn

© 2025 Chinese Physical Society and IOP Publishing Ltd. All rights, including for text and data mining, AI training, and similar technologies, are reserved.

tocol is general and can be combined with the most existing DD sequences. Especially, we find that our protocol can significantly suppress the Rabi error. We also apply our protocol on quantum lock-in detection for highly robust quantum sensing. And our protocol has broad application prospect in magnetometer,[26,31,34–36] atomic clocks,[37–39] gravimeter,[40] gyroscope,[41] and so on.[10,33,42]

This article is organized as follows. In Section 2, we introduce our general protocol of phase-modulated dynamical decoupling sequences. We demonstrate the robustness of our protocol. In Section 3, we apply our protocol to quantum sensing. We demonstrate how to achieve the robust quantum lock-in detection for alternating signals estimation. Finally, we give a brief summary in Section 4.

2. The phase-modulated dynamical decoupling sequences

In general, a DD sequence is consistent of many π pulses. For a two-level system such as NV center[29,43–45] and single trapped ion,[28] its energy levels are labeled by $|\uparrow\rangle$ and $|\downarrow\rangle$, and can be described via the Pauli operators $\hat{\sigma}_{x,y,z}$. The control Hamiltonian of a sequence of π pulses can be written as

$$\hat{H}_{\rm ctrl}(t) = \hbar\Omega(t)[\cos(\phi(t))\hat{\sigma}_x + \sin(\phi(t))\hat{\sigma}_y]/2 \tag{1}$$

with

$$\Omega(t) = \begin{cases} \pi/T_\Omega, & |t-t_j| \le T_\Omega/2, \\ 0, & \text{others}, \end{cases} \tag{2}$$

and the pulse phase

$$\phi(t) = \begin{cases} \phi_j, & |t-t_j| \le T_\Omega/2, \\ 0, & \text{others}. \end{cases} \tag{3}$$

Ideally, the π pulse is hard with $T_\Omega \to 0$. In realistic experiments, limited by the Rabi frequency Ω, there is the pulse length $T_\Omega \neq 0$. Without loss of generality, we suppose a π pulse with phase $\phi(t_j) = \phi_j$ is applied at time node t_j $(j = 1,2,\ldots,n)$ (see Fig. 1(a)). DD sequences with different pulse phases or the pulse intervals have been proposed, such as the UDD sequences have the same pulse phase (i.e., $\phi_j = 0$), while have different pulse intervals (i.e., $(t_j - t_{j-1})$),

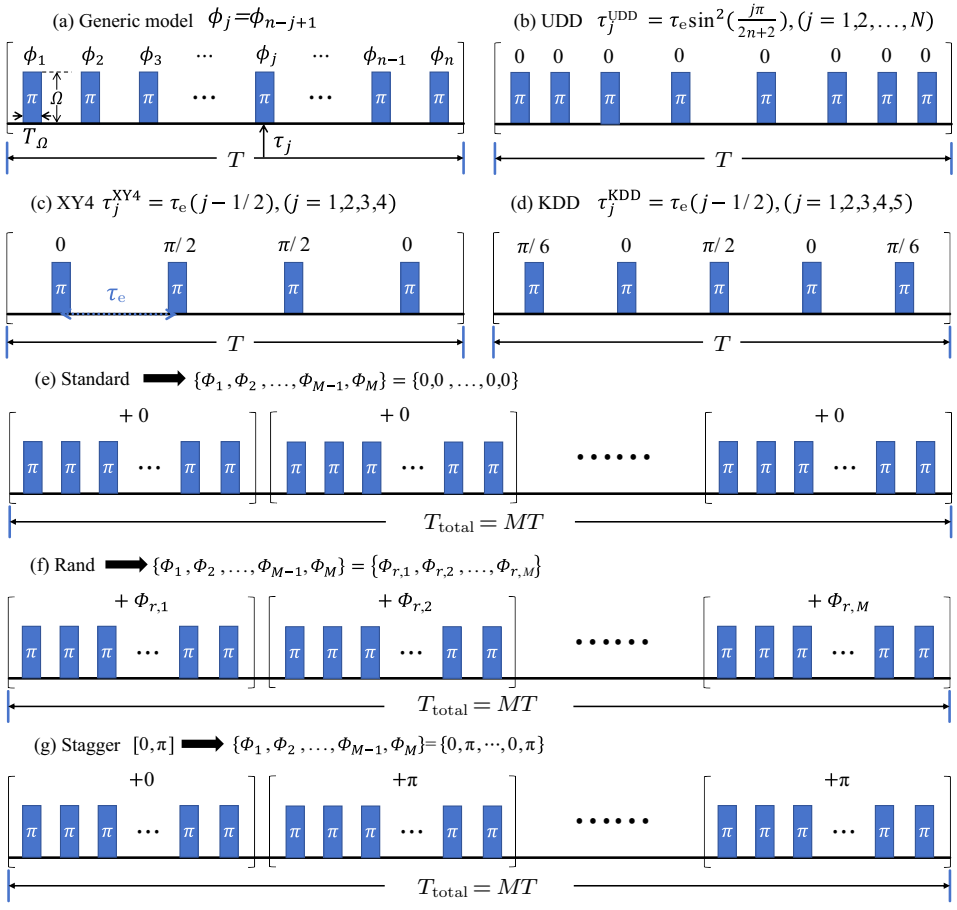


Fig. 1. Dynamical decoupling sequence composed of π pulses. (a) The generic model of DD sequences. A π pulse with phase ϕ_j is applied at time node t_j $(j = 1,2,\ldots,n)$. For most sequences, we have $\phi_j = \phi_{n-j+1}$. Considering the real experimental system, limited by the Rabi frequency Ω, we define the pulse length as T_Ω. (b) The π pulses of UDD sequence have the same $\phi_j = 0$ while have different pulse intervals $(t_j - t_{j-1})$. (c) The XY4 and (d) KDD sequences have the same pulse interval $(t_j - t_{j-1})$ while have different pulse phases ϕ_j. (e) Standard way to construct a longer sensing sequence by repeating the same basic pulse unit in (a) M times. The global phase imposed on the m-th unit is $\Phi_m = \Phi$, (f) phase randomization protocol shifting all the pulses within each unit by a common random phase $\Phi_{{\rm r},m}$ at different blocks is independent. (g) The staggered sequence $\{\Phi_1,\Phi_2,\ldots,\Phi_{{\rm r},M-1},\Phi_{{\rm r},M}\} = \{0,\pi,\ldots,0,\pi\}$ (M is even) of the randomization protocol when each unit is symmetry, i.e., $\phi_j = \phi_{n-j+1}$.

see Fig. 1(b). However, the XY(4,8,16,...)[13] sequences and KDD sequences[13,24,25] have the same pulse interval $\tau_e = t_j - t_{j-1}$ while have different phases, see Figs. 1(c) and 1(d). Moreover, to realize more robust protocol, the authors in Ref. [13] proposed a phase randomization protocol. The phase randomization protocol is achieved by, first, adding a global phase to the applied π pulses within one elemental unit and, second, randomly changing this phase each time the unit is repeated (see Fig. 1(f)). And the simplified randomization protocol does not change the global phase, just repeats the same basic pulse, which is called standard protocol, as shown in Fig. 1(e).

Now we illustrate our phase-modulated dynamical decoupling sequences. Based on the idea of phase randomization protocol of DD sequences, our protocal contains M repetitions of the basic DD unit (see Fig. 1(e)). Considering the Rabi error and detuning,[13,25] the Hamiltonian of a sequence of π pulses in our protocol becomes (see Appendix A for more details)

$$\hat{H}(\epsilon,\Delta) = \Omega(t)(1+\epsilon)\hat{\sigma}_{m,j}/2 + \Delta\hat{\sigma}_z/2 \tag{4}$$

with

$$\hat{\sigma}_{m,j} = \cos(\Phi_m+\phi_j)\hat{\sigma}_x + \sin(\Phi_m+\phi_j)\hat{\sigma}_y. \tag{5}$$

Here, ϵ denotes the Rabi error, Δ denotes the detuning. Global phases Φ_m is imposed on all the pulses within the m-th unit ($m = 1,2,\ldots,M$ where M is even), as shown in Figs. 1(e)–1(g). In general, the robustness of a DD sequences against systemic errors varies with global phases $\{\Phi_m\}$.[13,24,46] Different from the phase randomization protocol of DD sequences, the global phases added to all the pulses of DD unit are 0 or π alternately, not a common random phase (see Fig. 1(g)).

To study the robustness of our protocol, one can use fidelity[47] to evaluate the DD sequence performance and it is[47]

$$F(\epsilon,\Delta) = \mathrm{Tr}[\hat{U}^\dagger(\epsilon,\Delta)\hat{U}(0,0)]/\mathrm{Tr}[\hat{U}^\dagger(0,0)\hat{U}(0,0)] \tag{6}$$

with

$$\begin{aligned}\hat{U}(\epsilon,\Delta) = &\prod_{m=1}^{M}\prod_{j=1}^{n}\exp\left(-\mathrm{i}\Delta\frac{\tau-T_\Omega}{2}\frac{\hat{\sigma}_z}{2}\right)\\ &\times\exp\left(-\mathrm{i}\pi(1+\epsilon)\frac{\hat{\sigma}_{m,j}}{2}-\mathrm{i}\Delta T_\Omega\frac{\hat{\sigma}_z}{2}\right)\\ &\times\exp\left(-\mathrm{i}\Delta\frac{\tau-T_\Omega}{2}\frac{\hat{\sigma}_z}{2}\right)\end{aligned} \tag{7}$$

and $\mathrm{Tr}[\hat{A}]$ means tracing $\hat{A}$. For convenience, we consider the fidelity with $\Delta = 0$. Thus, we have

$$\hat{U}(\epsilon,0) = \prod_{m=1}^{M}\prod_{j=1}^{n}\exp\left(-\mathrm{i}\pi(1+\epsilon)\frac{\hat{\sigma}_{m,j}}{2}\right). \tag{8}$$

Here, we assume $\{\Phi_m\} = \{0,\pi,\ldots,0,\pi\}$ and utilize $\cos(\phi_j+\pi)\hat{\sigma}_x + \sin(\phi_j+\pi)\hat{\sigma}_y = -[\cos(\phi_j)\hat{\sigma}_x + \sin(\phi_j)\hat{\sigma}_y]$, one can have

$$\hat{U}(\epsilon,0) = \hat{U}(0,0). \tag{9}$$

That means the Rabi error has no effect at all on our phase-modulated DD sequences. In the Bloch sphere, the unitary operation $\hat{U}(\epsilon,0)$ is equivalent to a state turning less $\epsilon\pi$ and earning more $\epsilon\pi$ along the same axis, which is equivalent to not turning. Hence, when choosing $\{\Phi_m\} = \{0,\pi,0,\pi,\ldots,0,\pi\}$ (see Appendix C for more details), one can obtain

$$\begin{aligned}&\hat{U}_{\mathrm{opt}}(\epsilon,0)\\ &= \left[\prod_{j=1}^{n}\exp\left(-\mathrm{i}\pi(1+\epsilon)\frac{-\hat{\sigma}_j}{2}\right)\prod_{j=1}^{n}\exp\left(-\mathrm{i}\pi(1+\epsilon)\frac{\hat{\sigma}_j}{2}\right)\right]^{M/2}\\ &= \left[\exp\left(\mathrm{i}\pi(1+\epsilon)\frac{\hat{\sigma}_n}{2}\right)\times\cdots\times\exp\left(\mathrm{i}\pi(1+\epsilon)\frac{\hat{\sigma}_1}{2}\right)\right.\\ &\quad\left.\times\exp\left(-\mathrm{i}\pi(1+\epsilon)\frac{\hat{\sigma}_n}{2}\right)\times\cdots\times\exp\left(-\mathrm{i}\pi(1+\epsilon)\frac{\hat{\sigma}_1}{2}\right)\right]^{M/2}\\ &= \left[\exp\left(\mathrm{i}\pi(1+\epsilon)\frac{\hat{\sigma}_1}{2}\right)\times\cdots\times\exp\left(\mathrm{i}\pi(1+\epsilon)\frac{\hat{\sigma}_n}{2}\right)\right.\\ &\quad\left.\times\exp\left(-\mathrm{i}\pi(1+\epsilon)\frac{\hat{\sigma}_n}{2}\right)\times\cdots\times\exp\left(-\mathrm{i}\pi(1+\epsilon)\frac{\hat{\sigma}_1}{2}\right)\right]^{M/2}\\ &= \mathcal{I}\end{aligned} \tag{10}$$

with $\hat{\sigma}_j = \cos(\phi_j)\hat{\sigma}_x + \sin(\phi_j)\hat{\sigma}_y$, $\phi_j = \phi_{n-j+1}$, and $\mathcal{I}$ denoting unit matrix. Substitutting Eq. (10) into Eq. (6), one can have $F(\epsilon,0) = 1$. Thus, our protocol can suppress the Rabi error absolutely.

Our protocol is general and can be combined with the most existing DD sequences with symmetric phase, i.e., $\phi_j = \phi_{n-j+1}$, such as XY-(4,8,16,...) sequences and KDD sequence. As shown in Figs. 2(a) and 2(e), we study the fidelity of $F(\epsilon,0)$ with different global phases for XY4 and KDD. We find the fidelity of our protocol is always 1 for both XY4 and KDD sequences being the same as Eq. (10). Thus our protocol can suppress the Rabi error absolutely for XY4 and KDD sequences when $\Delta = 0$. We also numerically calculate the fidelity of $F(\epsilon,\Delta)$ for different DD sequences. According to our result, we find that our protocol has the most yellow areas representing the highest fidelity in the vicinity of the center point ($\epsilon = 0, \Delta = 0$) (see Appendix E for more details), as shown in Fig. 2. The increasing size of this yellow area demonstrates the improvement in error tolerance of our protocol in the vicinity of the center point.[48] Thus our protocol has the best robustness in our consideration.

Moreover, due to the fact that the global phases do not change the internal structure (i.e., the relative phases among π pulses) of the basic unit, the robustness of the basic DD sequence still can be preserved in our protocol. To show the application of our protocol in quantum sensing, in the following, we utilize our scheme for quantum lock-in detection as an example.

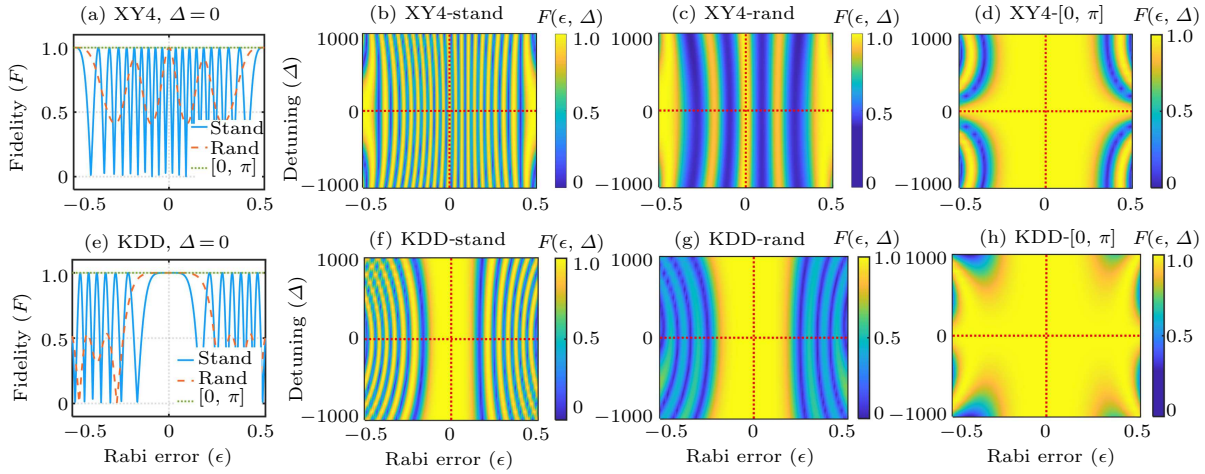


Fig. 2. Fidelity $F(\epsilon,\Delta)$ of XY4 and KDD sequences as a function of Rabi frequency error ϵ and detuning Δ. (a) Fidelity of XY4 sequences as a function of Rabi frequency errors $F(\epsilon,0)$ for the standard $\Phi_m = 0$ (blue solid line), a random randomization $\{\Phi_{r,m}\} = \{5.47, 0.31, 0.53, 3.17, 3.15, 1.37, 2.77, 4.66, 2.36, 2.06\}$ (red dashed line), and the alternation $\{\Phi_m\} = \{0, \pi, \ldots, 0, \pi\}$ (green dotted line) without detuning ($\Delta = 0$). (b)–(d) Fidelity $F(\epsilon,\Delta)$ of XY4 sequences as a function of Rabi frequency error ϵ and detuning Δ for the standard (XY4) (b), the randomization (RXY4) (c), and the alternation ($[0,\pi]$) (d). (e) Fidelity of KDD sequences as a function of Rabi frequency errors $F(\epsilon,0)$ for the standard (blue solid line), a random randomization $\{\Phi_{r,m}\} = \{2.37, 5.66, 2.92, 0.74, 1.55, 5.72, 3.77, 2.88\}$ (red dashed line), and the alternation (green dotted line) without detuning. (f)–(i) Fidelity $F(\epsilon,\Delta)$ of KDD sequences as a function of Rabi frequency error ϵ and detuning Δ for the standard (KDD) (f), the randomization (RKDD) (g), and the alternation ($[0,\pi]$) (h). Here, we choose pulse number $Mn = 80$ for both XY4 ($n = 4$) and KDD ($n = 5$) sequences.

3. Robust quantum lock-in measurement

Precision magnetic field measurements is an essential task in both fundamental physics[49–53] and practical applications.[54–57] Quantum lock-in detection is an essential technique in quantum metrology, which can be used to extract alternating signals from noise by employing dynamic decoupling to mitigate the influence of unwanted spectral components. In this section, we illustrate how to use our protocol to realize a quantum lock-in detection with robustness against systematic errors.

In general, quantum lock-in detection can be realized via quantum interferometry under a periodic multipulse sequence[28,31,47,58,59] to extract the weak alternating signal $S(t) = S_0\cos(\omega t) = \gamma_e B_{ac}\cos(\omega t)$ with the gyromagnetic ration γ_e and the target magnetic field amplitude B_{ac}. The coupling between the probe and the external signal is described by the Hamiltonian (see Fig. 3(a))

$$\hat{H}_{int} = \frac{\hbar}{2}S(t)\hat{\sigma}_z. \tag{11}$$

Further, to implement the quantum lock-in detection, one can use the DD pulse sequence as an reference signal and it can be written as Eq. (1). Under the DD sequences, we have $\tilde{\hat{A}}(t) = \hat{U}^\dagger(t)\hat{A}\hat{U}(t)$ with $\hat{U}(t) = \hat{\mathcal{T}}\int_0^t \hat{H}_{ctrl}(t')\mathrm{d}t'$ and $\hat{\mathcal{T}}$ is the time-ordering operator. Especially, if the operator $\hat{A} = \hat{\sigma}_z$, one can obtain $\tilde{\hat{\sigma}}_z = F_z(t)\hat{\sigma}_z + F_x\hat{\sigma}_x + F_y\hat{\sigma}_y$ with

$$F_\mu = \frac{1}{2}\mathrm{Tr}(\tilde{\hat{\sigma}}_z\hat{\sigma}_\mu), \tag{12}$$

where $\mathrm{Tr}(\hat{X})$ is the trace of matrix $\hat{X}$. After some algebras, the Hamiltonian $\hat{H}_I$ in the interaction picture of the DD pules sequence $\hat{H}_{ctrl}$ can be written as (see Appendix D for more details)[13]

$$\hat{H}_I(t) = \frac{\hbar}{2}F_z(t)S(t)\hat{\sigma}_z + \frac{\hbar}{2}S(t)\left(F_x\hat{\sigma}_x + F_y\hat{\sigma}_y\right), \tag{13}$$

with $F_\mu = \frac{1}{2}\mathrm{Tr}(\tilde{\hat{\sigma}}_z\hat{\sigma}_\mu)$ $(\mu = x,y,z)$. In our consideration of the pulse length T_Ω, we choose the DD sequence as

$$\Omega(t,T_\Omega) = \begin{cases} \pi/T_\Omega, & |t-(j-1/2)\tau_e| < T_\Omega/2, \\ 0, & \text{others}, \end{cases} \tag{14}$$

where $j = 1,2,\ldots,N$ $(N = nM)$ denotes the pulses number and T_Ω denotes the pulse length. For ideal pulses $T_\Omega = 0$, $F_\perp(t) = 0$ (see Figs. 1(c) and 1(d)), the interaction Hamiltonian can be simplified as

$$\hat{H}_I = \frac{\hbar}{2}S(t)F_z(t)\hat{\sigma}_z, \tag{15}$$

with $F_z(t)$ is filter function and it is

$$F_z(t) = \begin{cases} 1, & 2j\tau_e \le t + 1/2\tau_e \le (2j+1)\tau_e, \\ -1, & (2j+1)\tau_e \le t + 1/2\tau_e \le 2(j+1)\tau_e. \end{cases} \tag{16}$$

Initializing the quantum system into the state $|\Psi(0)\rangle = (|\uparrow\rangle + |\downarrow\rangle)/\sqrt{2}$, the instantaneous state in the interaction picture at time $t_N = N\tau_e = nM\tau_e$ becomes

$$|\Psi(t_N)\rangle_I = (e^{-i\varphi_N/2}|\uparrow\rangle + e^{i\varphi_N/2}|\downarrow\rangle)/\sqrt{2} \tag{17}$$

with $\varphi_N = \int_0^{t_N} F_z(t)S(t)\,\mathrm{d}t$. Especially, one can choose an even pulses number N to suppress DC noise due to $\int_0^{t_N} F_z(t)\,\mathrm{d}t = 0$.[49] The role of a quantum lock-in detection is to tailor $F_z(t)$ synchronized with the target signal $S(t)$, allowing the phase accumulation coherently owing to $S(t)$. Finally, a unitary operation $e^{-i\frac{\pi}{4}\hat{\sigma}_x}$ ($\pi/2$ pulse along x axis) is applied for readout, the population difference between the states $|\uparrow\rangle$ and $|\downarrow\rangle$ reads

$$\langle\hat{\sigma}_z\rangle_N = \sin(\varphi_N). \tag{18}$$

For CPMG sequence, XY4 sequence, and KDD sequence, we

have

$$\varphi_N = \frac{2S_0}{\omega}\cos\left[\frac{N\omega\cdot(\tau_e-\tau)}{2}\right] \times\left[1+\sin\left(\frac{\omega\cdot(\tau_e-\tau)}{2}\right)\right]\frac{\sin[N\omega\cdot(\tau_e-\tau)/2]}{\sin[\omega\cdot(\tau_e-\tau)/2]}. \quad (19)$$

Here, $\tau=\pi/\omega$ is the half-period of the target signal. Obviously, φ_N is the antisymmetric phase with respect to the lock-in point $\tau_e=\tau$. Moreover, if $2S_0N/\omega\ll 1$, we have $\langle\hat{\sigma}_z/2\rangle_N\approx\varphi_N/2$.[29,30] Thus, one may determine the lock-in point from the pattern symmetry by modulating the pulse repetition period τ_e.

However, in realistic situations, the π pulses are not instantaneous due to limited light power, so the function $F_\perp(t)$ has a nonzero value during π pulse execution and $F_z(t)$ deviates from ±1[13] (Figs. 1(c) and 1(d)). The presence of nonzero $F_\perp(t)=F_x(t)+\mathrm{i}F_y(t)$ may alter the expected signal or cause spurious peaks to appear. In our study, we find that the Rabi error and the detuning will affect the measurement results,[59] as shown in Figs. 3(b) and 3(f). Further, we study the relative deviation of the amplitude S_0 for the different amplitude error ϵ and detuning Δ. We define the relative deviation of the amplitude as $\delta/A=|B_{ac}^{est}-B_{ac}|/B_{ac}$. As shown in Figs. 3(c), 3(d), 3(e), 3(g), 3(h), and 3(i), we numerically calculate the relative deviation δ/A for different XY4 and KDD sequences. Compared with previous protocols, we find our protocol improves the relative error of measurement results by orders of magnitude, as shown in Fig. 3. Thus our protocol can enhance the performance of quantum lock-in detection for quantum sensing.

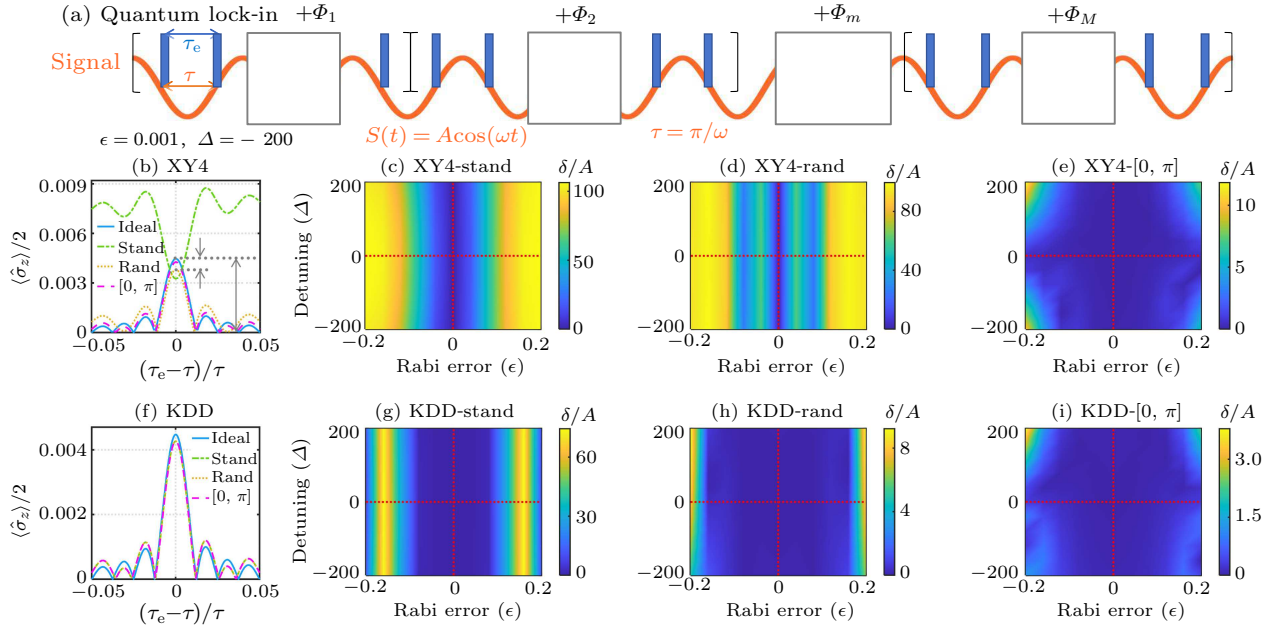


Fig. 3. The robustness of our protocol in quantum lock-in detection. (a) Quantum lock-in detection scheme. (b) Quantum lock-in signal $\langle\hat{\sigma}_z/2\rangle$ with XY4 sequences for the standard $\Phi_m=0$ (green dash-dotted line), a random randomization $\{\Phi_{r,m}\}=\{5.47,0.31,0.53,3.17,3.15,1.37,2.77,4.66,2.36,2.06\}$ (orange dotted line), and the alternation $\Phi_m=\{0,\pi,\ldots,0,\pi\}$ (purple dashed line) with $\epsilon=-0.001$, $\Delta=-200$ and all XY4 sequences results without error (blue solid line). (c)–(e) The magnetic field amplitude measurement relative error δ/A at the lock-in point $\tau_e=\pi/\omega$ for XY4 (c), RXY4 (d), and XY4-$[0,\pi]$ (e). (f) Quantum lock-in signal $\langle\hat{\sigma}_z/2\rangle$ with KDD sequences for the standard $\Phi_m=0$ (green dash-dotted line), the randomization (orange dotted line), and the alternation (purple dashed line) with $\epsilon=-0.001$, $\Delta=-200$, and all KDD sequences results without error (blue solid line). (f)–(h) The magnetic field amplitude measurement relative error δ/A at the lock-in point $\tau_e=\pi/\omega$ for KDD $\Phi_m=0$ (f), RKDD $\{\Phi_{r,m}\}=\{2.37,5.66,2.92,0.74,1.55,5.72,3.77,2.88\}$ (g), and the alternation $[0,\pi]$ (h). Here, the gyro-magnetic ration $\gamma_e=2\times\pi\times2802400$ Hz/Gs (Yb^+_{171}), the target magnetic field amplitude is 10^{-8} Gs (1 Gs = 10^{-4} T), frequency $\omega=100\pi$, pulse length $T_\Omega=0.1\tau$, and pulse number $Mn=80$.

4. Discussion and conclusion

We theoretically propose a robust phase-modulated dynamical decoupling sequences to suppress systemic errors, which is based on the idea of phase randomization protocol of DD sequences, the differences are the global phase added to all the pulses of DD unit being 0 or π alternately, not a common random phase. On the basis of our protocol, we find that our protocol can significantly reduce the Rabi error. Compared with the most existing DD sequences, our protocol also can suppress detuning mostly. In addition to varying the global phases appended to the pulses in the dynamical decoupling unit alternatively with 0 or π, we find that for $M=4k$ ($k=1,2,3,\ldots$) repetitions of the basic DD unit, varying the global phases with $[0,\pi,\pi,0]$ have a better error tolerance (see Appendix C for numerical results).

Furthermore, we also numerically demonstrated that our protocol can be used in a quantum lock-in detection to measure ac signal. After some numerical calculation, we find the relative errors of our protocol are smaller than the standard protocol and the randomization protocol's, especially for weak signal. Our protocol is general and can be combined with the most existing DD sequences, such as XY(4,8,16,...) sequences, KDD sequences, UDD sequences, and so on. Thus it is simple to implement in many two-level experimental sys-

tems, such as NV centers, trapped ions, and so on which can even be applied in many-body entanglement system to achieve high precision and high robustness metrology.[31,60] In addition to the Rabi error and detuning, the robustness of our protocol to other common experimental noises (such as phase noise and temperature drift) is also important and can be studied in the future. Considering the global phases does not change the internal structure of the basic unit, our protocol still is robust to the other common experimental noises.[13,27] Our study may pave a simple and feasible way to realize robust DD sequences, and achieve robust quantum lock-in detection for quantum sensing. And our protocol is widely used in many diverse fields, ranging from fundamental physics,[38,61–63] geographic metrology[64,65] to material science,[26,66] and biomedical sensing.[67–69]

Appendix A: Modulation function of dynamical decoupling sequence

Usually, a DD sequence can be generated by a sequence of microwave pulses[13] or optical pulses[70] whose Hamiltonian is

$$\hat{H}_{\rm DD} = \Omega(t)\cos[\omega_{\rm p}t+\phi(t)]\hat{\sigma}_x \tag{A1}$$

with $\omega_{\rm p}$ is the coupling field angle frequency. The two-level system internal Hamiltonian is $\hat{H}_0 = \omega_0\hat{\sigma}_z/2$ with the energy difference ω_0 between $|\uparrow\rangle$ and $|\downarrow\rangle$, hence the whole Hamiltonian is

$$\hat{H} = \omega_0\hat{\sigma}_z/2+\Omega(t)\cos[\omega_{\rm p}t+\phi(t)]\hat{\sigma}_x. \tag{A2}$$

Usually, we have $\omega_0 \gg |\Delta|$ with the detuning $\Delta = \omega_0-\omega_{\rm p}$. In the interaction picture with respecting to $\omega_{\rm p}\hat{\sigma}_z/2$, the time-evolution obeys

$$\mathrm{i}\frac{\partial|\Psi(t)\rangle_{\rm I}}{\partial t} = \frac{1}{2}H_{\rm I}|\Psi(t)\rangle_{\rm I} \tag{A3}$$

with

$$\hat{H}_{\rm I} = \Delta\hat{\sigma}_z/2+\Omega(t)\left[\cos(\phi(t))\hat{\sigma}_x+\sin(\phi(t))\hat{\sigma}_y\right]/2, \tag{A4}$$

which is Eq. (4) in the main text after rotating wave approximation (RWA). Under the $\hat{H}_{\rm ctrl}$ scene, we have $\tilde{\hat{A}}(t) = \hat{U}^\dagger(t)\hat{A}\hat{U}(t)$ with $\hat{U}(t) = \hat{\mathcal{T}}\int_0^t\hat{H}_{\rm I}(t')\,\mathrm{d}t'$ and $\hat{\mathcal{T}}$ is the time-ordering operator. Specially, if the operator $\hat{A}$ is the angular momentum operator $\hat{\sigma}_z/2$, one can obtain $\tilde{\hat{\sigma}}_z/2 = F_z(t)\hat{\sigma}_z/2+F_x(t)\hat{\sigma}_x/2+F_y(t)\hat{\sigma}_y/2$ and $F_\perp = F_x+\mathrm{i}F_y$. Hence we can easily obtain

$$F_\mu = \frac{1}{2}\mathrm{Tr}(\tilde{\hat{\sigma}}_z\hat{\sigma}_\mu), \tag{A5}$$

where $\mathrm{Tr}(\hat{X})$ is the trace of matrix $\hat{X}$.

For a sequence of π pulses, if a π pulse is applied at time t_j, the evolution driven by $\hat{H}_{\rm I}$ reads $\hat{P}_j(\theta) = \mathrm{e}^{-\mathrm{i}\theta\left[\cos(\phi_j)\hat{\sigma}_x/2+\sin(\phi_j)\hat{f}_y\right]}$, where $\theta = \theta(t) = \pi(t-t_j-T_\Omega/2)/T_\Omega \in [0,\pi]$ is the angle of rotation and $\phi_j = \phi(t_j)$. Defining $\hat{P}_j(\theta) = \hat{P}_j(\pi)$ as the propagator of a single π pulse, one can obtain the propagator for $2j+1$ $(j=0,1,\ldots)$ pulses

$$\begin{aligned}\hat{U}_{2j+1} &= \hat{P}_{2j+1}\hat{P}_{2j}\cdots\hat{P}_2\hat{P}_1\\ &= 2(-1)^{j+1}\sin(\Phi_{2j+1})\hat{\sigma}_x/2\\ &\quad -2(-1)^{j+1}\cos(\Phi_{2j+1})\hat{f}_y,\end{aligned} \tag{A6}$$

and for $2j$ pulses

$$\hat{U}_{2j} = \hat{P}_{2j}\cdots\hat{P}_1 = (-1)^j\mathrm{e}^{-2\mathrm{i}\Phi_{2j}\hat{\sigma}_z/2}, \tag{A7}$$

where $\Phi_k = \sum_{l=1}^k(-1)^l\phi_l$. According to Eqs. (A5)–(A7), we can obtain the modulation functions as follows:

$$F_z(t) = (-1)^{j-1}\cos(\theta), \tag{A8}$$

$$F_\perp(t) = i(-1)^{j-1}\mathrm{e}^{-\mathrm{i}(\Phi_{j-1}+\Phi_j)}\sin(\theta). \tag{A9}$$

Because $\theta = \theta(t)$ in Eqs. (A8) and (A9) is the pulse area that the j-th pulse has rotated at the moment t, for ideal pulses $(T_\Omega \to 0)$, $F_\perp(t)$ has no effect (because $\sin(\theta) = 0$ for all time t) and $F_z \in \{\pm 1\}$. However, in the realistic case, the pulses are not instantaneous $(T_\Omega > 0)$, $F_\perp(t)$ is non-zero during the π pulses. And the $F_\perp(t)$ varies with the phases $\{\phi_j\},\{\Phi_m\}$ for the same $T_\Omega > 0$.

Appendix B: Filter function of dynamical decoupling sequence

The filter function is actually the frequency domain representation of the modulation function F_μ,[13,49] i.e., the Fourier transform of the modulation function

$$f_k^\mu = \frac{1}{MT}\int_0^{MT}F_\mu(t)\exp\left(-\mathrm{i}\frac{2\pi kt}{MT}\right)\mathrm{d}t. \tag{B1}$$

Under the randomization protocol, a random phase $\Phi_{{\rm r},m}$ $(m = 1,2,\ldots,M)$ is added to all pulses in the m-th repetition of the basic unit. These random phases do not affect $F_z(t)$ but alter $F_\perp(t)$ to $F_{r,\perp}(t) = F_\perp(t)\mathrm{e}^{\mathrm{i}\Phi_{{\rm r},m}}$. And we have

$$\begin{aligned}f_k^\perp &= \frac{1}{MT}\int_0^{MT}F_{r,\perp}(t)\exp\left(-\mathrm{i}\frac{2\pi kt}{MT}\right)\mathrm{d}t\\ &= \frac{1}{MT}\sum_{m=1}^{M}\int_{(m-1)T}^{mT}F_\perp(t)\mathrm{e}^{\mathrm{i}\Phi_{{\rm r},m}}\exp\left(\left(-\mathrm{i}\frac{2\pi kt}{MT}\right)\right)\mathrm{d}t\\ &= Z_{r,k,M}\tilde{f}_{k/M}^\perp,\end{aligned} \tag{B2}$$

where

$$Z_{r,k,M} = \frac{1}{M}\sum_{m=1}^{M}\mathrm{e}^{\mathrm{i}[\Phi_{{\rm r},m}-2\pi k(m-1)/M]},$$

$$\tilde{f}_{k/M}^\perp = \frac{1}{T}\int_0^T F_\perp(t)\exp\left(-\mathrm{i}\frac{2\pi kt}{MT}\right)\mathrm{d}t.$$

For the randomization protocol in Ref. [13], considering $\Phi_{{\rm r},m}$ is random and hence $\Phi_{{\rm r},m}-2\pi k(m-1)/M$ is also random, one can obtain $Z_{r,M} = \frac{1}{M}\sum_{m=1}^{M}\exp(\mathrm{i}\Phi_{{\rm r},m})$. And then the correlated randomization protocol is proposed by Wang *et al.*[27] However, for difference random digit $\{\Phi_{{\rm r},m}\}$, the fidelity which characterizes the DD sequence performance is different as shown in Fig. 2. And we have found the optimial $\{\Phi_{{\rm r},m}\}$ for symmetric DD sequence whose fidelity is always 1 when $\Delta = 0$.

Appendix C: The robustness enhancement of optimized randomization protocol

In this section, we will discuss the robustness enhancement of our protocol and we concentrate on the Rabi frequency control error. Compared with Ref. [13], we ignore the influence of detuning and phase error because their robustness has been improved obviously in the random scheme especially the detuning has almost even no effect on the standard model. The evolution driven by the single j-th π pulse with Rabi error takes the general form

$$\hat{U}_{s,j}(\epsilon) = \mathrm{e}^{-\mathrm{i}\pi(1+\epsilon)/2(\cos\phi_j\hat{\sigma}_x+\sin\phi_j\hat{\sigma}_y)} = \begin{pmatrix} -\sin(\epsilon\pi/2) & -\mathrm{i}\cos(\epsilon\pi/2)\mathrm{e}^{-\mathrm{i}\phi_j} \\ -\mathrm{i}\cos(\epsilon\pi/2)\mathrm{e}^{\mathrm{i}\phi_j} & -\sin(\epsilon\pi/2) \end{pmatrix}, \quad \text{(C1)}$$

where ϵ is the relative Rabi error. Here, we assume that each pulse has the same ϵ, and equation (C1) describes a perfect π pulse when $\epsilon = 0$. Consider a basic unit with N π pulses applied at t_j ($j = 1,2,\ldots,N$) with phases ϕ_j. And we have the propagator of a basic pulse unit

$$\hat{U}_{\mathrm{unit}} = \hat{U}_{s,N}\hat{U}_{s,N-1}\cdots\hat{U}_{s,2}\hat{U}_{s,1}. \quad \text{(C2)}$$

When one adds a random global phase $\Phi_{\mathrm{r},m}$ on all the π pulses in a basic DD unit, each $\hat{U}_{s,j}(\epsilon)$ in the m-th block becomes

$$\hat{U}_{s,j,m}(\epsilon) = \begin{pmatrix} \sin(\epsilon\pi/2) & -\mathrm{i}\cos(\epsilon\pi/2)\mathrm{e}^{-\mathrm{i}(\phi_j+\Phi_{\mathrm{r},m})} \\ -\mathrm{i}\cos(\epsilon\pi/2)\mathrm{e}^{\mathrm{i}(\phi_j+\Phi_{\mathrm{r},m})} & \sin(\epsilon\pi/2) \end{pmatrix}. \quad \text{(C3)}$$

The robustness can be described by the fidelity $\mathrm{Tr}[\hat{U}_M^\dagger(\epsilon)\hat{U}_M(\epsilon=0)]/\mathrm{Tr}[\hat{U}_M^\dagger(\epsilon=0)\hat{U}_M(\epsilon=0)]$. Moreover, if there are detuning Δ, each $\hat{U}_{s,j}(\epsilon)$ in the m-th block becomes

$$\hat{U}_{s,j,m}(\epsilon,\Delta) = \exp\left(-\mathrm{i}\Delta\frac{\tau-T_\Omega}{2}\frac{\hat{\sigma}_z}{2}\right)\exp\left(-\mathrm{i}\pi(1+\epsilon)\frac{\hat{\sigma}_{m,j}}{2}-\mathrm{i}\Delta T_\Omega\frac{\hat{\sigma}_z}{2}\right)\exp\left(-\mathrm{i}\Delta\frac{\tau-T_\Omega}{2}\frac{\hat{\sigma}_z}{2}\right) \quad \text{(C4)}$$

with $\hat{\sigma}_{m,j} = \begin{pmatrix} 0 & \mathrm{e}^{-\mathrm{i}(\phi_j+\Phi_{\mathrm{r},m})} \\ \mathrm{e}^{\mathrm{i}(\phi_j+\Phi_{\mathrm{r},m})} & 0 \end{pmatrix}$. And we can judge its robustness by the fidelity Eq. (6).

In the main text, we have shown that our protocol has the best robustness against the Rabi error when $|\Delta| \leq 1000$.

However, when Δ is large, we find a new sequence $[0,\pi,\pi,0]$ with more symmetries being better than $[0,\pi]$ which has a larger yellow area as shown in Fig. C1.

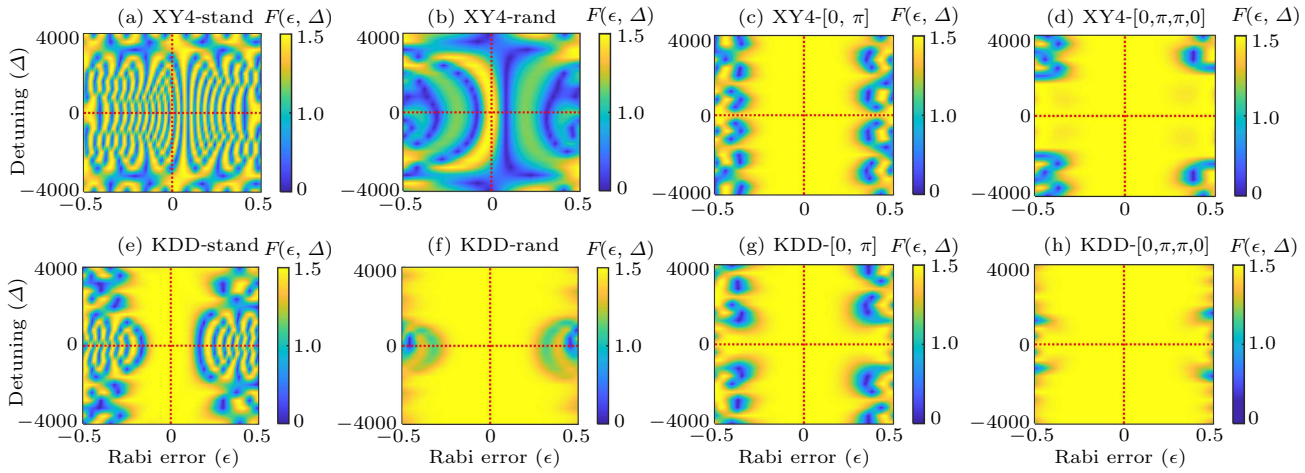


Fig. C1. Fidelity $F(\epsilon,\Delta)$ of XY4 and KDD sequences as a function of Rabi frequency error ϵ and detuning Δ. (a)–(d) Fidelity $F(\epsilon,\Delta)$ of XY4 sequences as a function of Rabi frequency error ϵ and detuning Δ for the standard (XY4) $\Phi_m = 0$ (a), the randomization (RXY4) $\{\Phi_{\mathrm{r},m}\} = \{5.47,0.31,0.53,3.17,3.15,1.37,2.77,4.66,2.36,2.06\}$ (b), the staggering ($[0,\pi]$) (c), and the new alternation ($[0,\pi,\pi,0]$) (d). (e)–(i) Fidelity $F(\epsilon,\Delta)$ of KDD sequences as a function of Rabi frequency error ϵ and detuning Δ for the standard (KDD) $\Phi_m = 0$ (e), the randomization (RKDD) $\{\Phi_{\mathrm{r},m}\} = \{2.37,5.66,2.92,0.74,1.55,5.72,3.77,2.88\}$ (f), and the optimized (KDD-$[0,\pi]$) (h), and the new alternating (KDD-$[0,\pi,\pi,0]$) (i). Here, we choose pulse number $N = Mn = 80$ for both XY4 and KDD sequences.

Appendix D: Quantum lock-in detection

In this section, we will give the derivation of Eq. (19). For a two-level single-particle system obeying the following Hamiltonian:

$$\hat{H} = \frac{\hbar}{2}\left[M(t)\hat{\sigma}_z + \Omega(t)[\cos(\phi(t))\hat{\sigma}_x + \sin(\phi(t))\hat{\sigma}_y]\right],$$

its Schrödinger equation can be written as

$$\mathrm{i}\frac{\partial|\Psi(t)\rangle_{\mathrm{S}}}{\partial t} = \frac{1}{2}[M(t)\hat{\sigma}_z + \Omega(t)[\cos(\phi(t))\hat{\sigma}_x + \sin(\phi(t))\hat{\sigma}_y]]|\Psi(t)\rangle_{\mathrm{S}}. \quad \text{(D1)}$$

Here, $M(t) = S(t) + N(t)$, and $S(t) = S_0\cos(\omega t)$ is the signal with the angle frequency ω and the amplitude A, and

$N(t)=\Delta$ is the detuning. In the interaction picture with respect to $\hat{H}_{\rm ref}=\frac{\hbar}{2}\Omega(t)[\cos(\phi(t))\hat{\sigma}_x+\sin(\phi(t))\hat{\sigma}_y]$, substituting $|\Psi(t)\rangle_{\rm S}=e^{-i/\hbar\int_0^t\hat{H}_{\rm ref}(t')dt'}|\Psi(t)\rangle_{\rm I}$ into Eq. (D1), the time-evolution of $|\Psi(t)\rangle_{\rm I}$ obeys

$$\begin{aligned}i\frac{\partial|\Psi(t)\rangle_{\rm I}}{\partial t}&=\frac{\hat{H}_{\rm I}}{\hbar}|\Psi(t)\rangle_{\rm I}\\&=(F_z(t)\hat{\sigma}_z+F_x(t)\hat{\sigma}_x+F_y(t)\hat{\sigma}_y)|\Psi(t)\rangle_{\rm I},\end{aligned}\tag{D2}$$

where F_z is Eq. (A8) and F_x+iF_y is Eq. (A9). At time t, the state $|\Psi(t)\rangle_{\rm I}$ becomes

$$\begin{aligned}|\Psi(t)\rangle_{\rm I}=\hat{\mathcal{T}}\exp\Bigg(-i\int_0^t\Big[&F_x(t')\hat{\sigma}_x+F_y(t')\hat{\sigma}_y\\&+F_z(t')\hat{\sigma}_z\Big]dt'\Bigg)|\Psi(0)\rangle_{\rm I},\end{aligned}\tag{D3}$$

where $\hat{\mathcal{T}}$ is the time-ordering operator.

In our protocol, we choose the reference signals as

$$\Omega(t,T_\Omega)=\begin{cases}\pi/T_\Omega, & |t-t_j|<T_\Omega/2,\\ 0, & \text{others},\end{cases}\tag{D4}$$

where T_Ω denotes the pulse length. For ideal pulses, the interaction Hamiltonian can be simplified as

$$\hat{H}_{\rm I}=\frac{\hbar}{2}S(t)F_z(t)\hat{\sigma}_z,\tag{D5}$$

where the filter function is given as

$$F_z(t)=\begin{cases}1, & 2j\tau_{\rm e}\le t+1/2\tau_{\rm e}\le(2j+1)\tau_{\rm e},\\ -1, & (2j+1)\tau_{\rm e}\le t+1/2\tau_{\rm e}\le 2(j+1)\tau_{\rm e}.\end{cases}\tag{D6}$$

Choosing each quantum system is initialized into $|\Psi\rangle_{\rm in}=\frac{|\uparrow\rangle+|\downarrow\rangle}{\sqrt{2}}$. At time t, the final state in the interaction picture is

$$\begin{aligned}|\Psi(t,\lambda)\rangle_{\rm I}&=\exp\left(-i\frac{\hat{\sigma}_z}{2}\int_0^t S(t')F_z(t',\lambda)dt'\right)|\Psi\rangle_{\rm in}\\&=\frac{|\uparrow\rangle+e^{i\phi_z(t,\lambda)}|\downarrow\rangle}{\sqrt{2}}.\end{aligned}\tag{D7}$$

For the results determined by the density matrix $\rho=|\Psi\rangle\langle\Psi|$, the global phase $e^{-i\varphi_N/2}$ can be ignored. The total accumulation phase $\phi_z(t)$ is

$$\phi_z(t)=\int_0^t S(t')F(t')dt'.\tag{D8}$$

In the Schrödinger picture,[28,31] the corresponding final state is

$$\begin{aligned}|\Psi(t)\rangle_{\rm S}&=\exp\left(-iF_z(t)\frac{\hat{\sigma}_x}{2}\right)|\Psi(t)\rangle_{\rm I}\\&=\frac{|\uparrow\rangle+e^{i(-1)^n\phi_z(t)}|\downarrow\rangle}{\sqrt{2}},\end{aligned}\tag{D9}$$

with the pulse number n, which is usually even. After a suitable unitary operation $U=e^{-i\frac{\pi}{4}\hat{\sigma}_y}$ for recombination,[31,71] the readout state is

$$\begin{aligned}|\Psi\rangle_{\rm re}(t)&=e^{i\phi_z'(t)/2}\left[-i\sin\left(\frac{\phi_z'(t)}{2}\right)|\uparrow\rangle+\cos\left(\frac{\phi_z'(t)}{2}\right)|\downarrow\rangle\right],\end{aligned}\tag{D10}$$

with $\phi_z'(t)=(-1)^n\phi_z(t)$ being the total accumulation phase under the Schrödinger picture.[28,31] Usually, n is even, hence the half probability difference between $|\uparrow\rangle$ and $|\downarrow\rangle$ is

$$\langle\hat{\sigma}_z/2\rangle(t)=\sin[\phi_z(t)]/2.\tag{D11}$$

Generally, one may consider how to obtain the target signal under two different situations, and determine the lock-in point from spectrum symmetry. Here, the two situations are considered: fixing the number of pulses and fixing the sensing time.

Firstly, we consider the situation of fixed pulse number $N_{\rm p}$. Substituting the target signal $S(t)=A\cos(\omega t)$ into Eq. (D8) and ignoring the noise $N(t)$, the phase accumulation at $t_n=n\tau_{\rm e}$ is

$$\begin{aligned}\varphi_N&=\phi_z(t_n)\\&=\int_0^{t_n}S_0\cos(\omega t')F_z(t')dt'\\&=\frac{S_0}{\omega}\int_0^{-\sin(\omega t_n)}F_z(t')d[\sin(\omega t')]\\&=\frac{S_0}{\omega}\sin(\omega t_n)\\&\quad+2\frac{S_0}{\omega}\sum_{j=1}^{n}\int_0^{t_n}(-1)^j\sin(\omega t')\delta\left[t'-(j-1/2)\tau_{\rm e}\right]dt'\\&=2\frac{S_0}{\omega}\cos\left[\frac{n\omega\cdot(\tau_{\rm e}-\tau)}{2}\right]\\&\quad\times\left[1+\sin\left(\frac{\omega\cdot(\tau_{\rm e}-\tau)}{2}\right)\right]\frac{\sin[n\omega\cdot(\tau_{\rm e}-\tau)/2]}{\sin[\omega\cdot(\tau_{\rm e}-\tau)/2]},\end{aligned}\tag{D12}$$

where $\tau=\pi/\omega$ is the half period of the target signal. According to Eq. (D12), the accumulated phase φ_N is symmetric to the lock-in point $(\tau_{\rm e}-\tau)/\tau=0$.[28,31] And the maximum value of the lock-in signal reflects the amplitude A of the target signal. Specially, if $S_0\ll\omega/2n$, we have $\langle\hat{\sigma}_z/2\rangle_{\max}\approx S_0n/\omega$. However, in experiments, there are Rabi errer ϵ and the error from detuning Δ with $\hat{H}=\frac{\hbar}{2}[(S(t)+\Delta)\hat{\sigma}_z+(1+\epsilon)\Omega(t)[\cos(\phi(t))\hat{\sigma}_x+\sin(\phi(t))\hat{\sigma}_y]]$, and the relative error of estimating A versus ϵ and Δ is shown in Fig. 3.

Appendix E: Quantitative analysis about error tolerance of different DD sequences

In this section, we will give a qualitative description to illustrate that our protocol is more robust than the standard and randomization protocol. To quantitatively analyze the error tolerance of different protocol based on XY4 and KDD sequences, we calculate the yellow area where the fidelity is higher than 0.95 in the vicinity of center point $(\epsilon=0,\Delta=0)$. As shown in Fig. E1, we give the contour line with fidelity of 0.95 near the center point in Fig. 2. The area within the contour line represents a fidelity higher than 0.95, and beyond the contour line, the fidelity begins to lower than 0.95.

After some calculations, the area of contour parcel areas are $\{16, 65, 1127, 425, 617, 1523\}$ for the standard (XY4) (a), the randomization (RXY4) (b), the alternation ($[0, \pi]$) (c), the standard (KDD) (d), the randomization (RKDD) (e), and the alternation ($[0, \pi]$) (f) respectively, see Fig. E1. Hence we can quantitatively analyze the error tolerance of different protocols based on XY4 and KDD sequences via the area of contour parcel areas which are $\{16, 65, 1127, 425, 617, 1523\}$ for the standard (XY4) (a), the randomization (RXY4) (b), and the alternation ($[0, \pi]$) (c), the standard (KDD) (d), the randomization (RKDD) (e), and the alternation ($[0, \pi]$) (f) respectively, see Fig. E1. Thus our protocol has the most yellow areas representing the highest fidelity in the vicinity of the center point ($\epsilon = 0, \Delta = 0$). Moreover, the increasing size of this yellow area demonstrates the improvement in error tolerance of our protocol in the vicinity of the center point. Thus our protocol has the best robustness in our consideration.

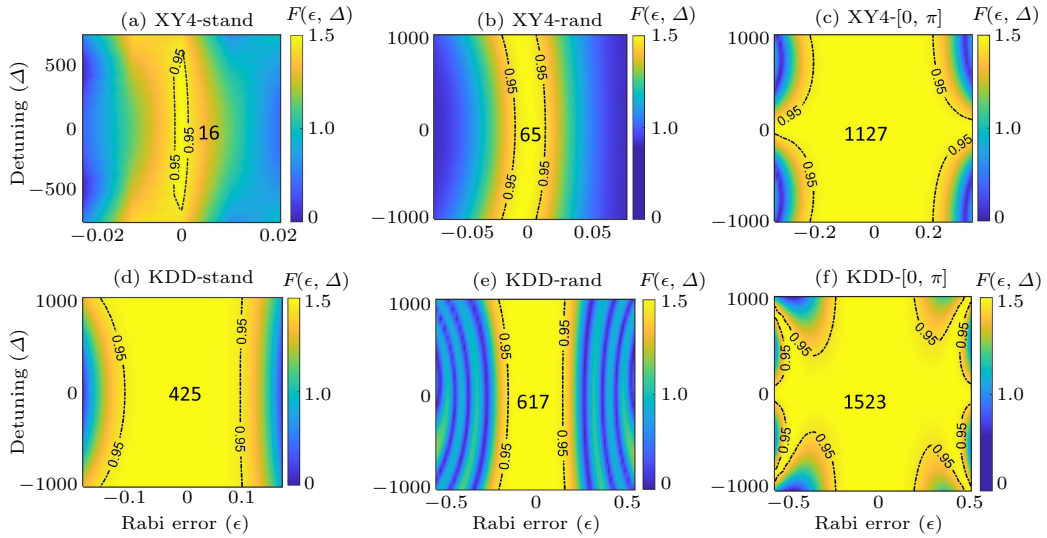


Fig. E1. Error tolerance of different protocols based on XY4 and KDD sequences. The contour line (black dashed-dotted line) with fidelity of 0.95 near the center point in Fig. 2. The area of contour parcel areas which are $\{16, 65, 1127, 425, 617, 1523\}$ for the standard (XY4) (a), the randomization (RXY4) (b), and the alternation ($[0, \pi]$) (c), the standard (KDD) (d), the randomization (RKDD) (e), and the alternation ($[0, \pi]$) (f) respectively. Here, we choose pulse number $Mn = 80$ for both XY4 ($n = 4$) and KDD ($n = 5$) sequences.

Acknowledgements

Project supported by the National Key Research and Development Program of China (Grant No. 2022YFA1404104), the National Natural Science Foundation of China (Grant Nos. 92476201, 12025509, 12305022, and 12475029), the Key-Area Research and Development Program of Guangdong Province, China (Grant No. 2019B030330001), and Guangdong Provincial Quantum Science Strategic Initiative Fund (Grant Nos. GDZX2305006 and GDZX2405002).

References

[1] Zhang J, Du P, Jing L and Xu P, You L and Zhang W 2024 *Chin. Phys. B* **33** 030301
[2] Sekiguchi Y, Komura Y and Kosaka H 2019 *Phys. Rev. Appl.* **12** 051001
[3] Liu G, Po H, Du J, Liu R and Pan X 2013 *Nat. Commun.* **4** 2254
[4] Pelzer L, Dietze K, Martínez-Lahuerta V J, Krinner L, Kramer J, Dawel F, Spethmann N C H, Hammerer K and Schmidt P O 2024 *Phys. Rev. Lett.* **133** 033203
[5] Barthel P, Huber P H, Casanova J, Arrazola I, Niroomand D, Sriarunothai T, Plenio M B and Wunderlich C 2023 *New J. Phys.* **25** 063023
[6] Hahn A, Burgarth D and Yuasa K 2022 *New J. Phys.* **24** 063027
[7] Connors E J, Nelson J, Edge L F and Nichol J M 2022 *Nat. Commun.* **13** 940
[8] Lijuan D, Inigo A, Xi C and Casanova J 2021 *Phys. Rev. Appl.* **15** 034055
[9] Zhang J and Suter D 2015 *Phys. Rev. Lett.* **115** 110502
[10] Bylander J, Gustavsson S, Yan F, Yoshihara F, Harrabi K, Fitch G, Cory D G, Nakamura Y, Tsai J and Oliver W D 2011 *Nat. Phys.* **7** 565
[11] Wang Y, Um M, Zhang J, An S, Lyu M, Zhang J, Duan L M, Yum D and Kim K 2017 *Nat. Photon.* **11** 646
[12] Wang P, Luan C, Qiao M, Um M, Zhang J, Wang Y, Yuan X, Gu M, Zhang J and Kim K 2021 *Phys. Rev. Lett.* **12** 233
[13] Wang Z, Lang J, Schmitt S, Lang J, Casanova J, McGuinness L, Monteiro T S, Jelezko F and Plenio M B 2019 *Phys. Rev. Lett.* **122** 200403
[14] Gong B, Tu T, Zhu X, Guo A, Zhou Z, Guo G and Li C 2020 *Sci. Rep.* **10** 15089
[15] Arrad G, Vinkler Y, Aharonov D and Retzker A 2014 *Phys. Rev. Lett.* **112** 150801
[16] West J R, Lidar D A, Fong B H and Gyure M F 2010 *Phys. Rev. Lett.* **105** 230503
[17] Álvarez G A and Suter D 2011 *Phys. Rev. Lett.* **107** 230501
[18] Merkel B, Fariña P C and Reiserer A 2021 *Phys. Rev. Lett.* **127** 030501
[19] Genov G T, Schraft D, Vitanov N V and Halfmann T 2017 *Phys. Rev. Lett.* **118** 133202
[20] Bazant P, Frydrych H, Alber G and Jex I 2015 *Phys. Rev. A* **92** 022325
[21] Qiu J, Zhou Y, Hu C, Yuan J, Zhang L, Chu J, Huang W, Liu W and Luo K 2021 *Phys. Rev. Appl.* **16** 054047
[22] Shim J H, Niemeyer I and Zhang J 2012 *Europhys. Lett.* **99** 40004
[23] Lang J E, Madhavan T, Tetienne J P, Broadway D A, Hall L T, Teraji T, Monteiro T S, Stacey A and Hollenberg L C L 2019 *Phys. Rev. A* **99** 012110
[24] Gupta1 M K, Navarro E J, Moulder T A, Mueller J D, Balouchi A, Brown K L, Lee H and Dowling J P 2015 *Phys. Rev. A* **91** 032329
[25] Souza A M, Álvarez G A and Suter D 2011 *Phys. Rev. Lett.* **106** 240501
[26] Lange G D, Wang Z H, Ristè D, Dobrovitski V V and Hanson R 2010 *Science* **330** 60
[27] Wang Z, Casanova J and Plenio M B 2020 *Symmetry* **12** 730
[28] Kotler S, Akerman N, Glickman Y, Keselman A and Ozeri R 2011 *Nature* **473** 61

[29] Schmitt S, Gefen T, Stürner F M, Unden T, Wolff G, Müller C, Scheuer J, Naydenov B, Markham M, Pezzagna S, Meijer J, Schwarz I, Plenio M, Retzker A, McGuinness L P and Jelezko F 2017 *Science* **356** 837
[30] Boss J M, Cujia K S, Zopes J and Degen C L 2017 *Science* **356** 837
[31] Zhuang M, Huang J and Lee C 2021 *PRX Quantum* **2** 040317
[32] Shibata K, Sekiguchi N and Hirano T 2021 *Phys. Rev. A* **103** 043335
[33] Shaniv R and Ozeri R 2017 *Nat. Commun.* **8** 14157
[34] Boross P, Széchenyi G and Pályi A 2018 *Phys. Rev. B* **97** 245417
[35] Parashar M, Bathla A, Shishir D, Gokhale A, Bandyopadhyay S and Saha K 2022 *Sci. Rep.* **12** 8743
[36] Hirose M, Aiello C D and Cappellaro P 2012 *Phys. Rev. A* **86** 062320
[37] McGrew W F, Zhang X, Fasano R J, Schäffer S A, Beloy K, Nicolodi D, Brown R C, Hinkley N, Milani G, Schioppo M, Yoon T H and Ludlow A D 2018 *Nature* **564** 87
[38] Dörscher S, Al-Masoudi A, Bober M, Schwarz R, Hobson R, Sterr U and Lisdat C 2020 *Commun. Phys.* **3** 185
[39] Aharon N, Spethmann N and Leroux I D 2019 *New J. Phys.* **21** 083040
[40] Stray B, Lamb A, Kaushik A, *et al.* 2022 *Nature* **602** 590
[41] Salducci C, Bidel Y, Cadoret M, Darmon S, Zahzam N, Bonnin A, Schwartz S, Blanchard C and Bresson A 2024 *Sci. Adv.* **10** 4498
[42] Almog I, Loewenthal G, Coslovsky J, Sagi Y and Davidson N 2016 *Phys. Rev. A* **94** 042317
[43] Wang G, Liu Y X, Zhu Y and Cappellaro P 2021 *Nano Lett.* **21** 5143
[44] Wang G, Liu X, Schloss J M, Alsid S T, Braje D A and Cappellaro P 2022 *Phys. Rev. X* **12** 021061
[45] Farfurnik D, Jarmola A, Pham L M, Wang Z H, Dobrovitski V V, Walsworth R L, Budker D and Bar-Gill N 2015 *Phys. Rev. B* **92** 060301
[46] Ryan C A, Hodges J S and Cory D G 2010 *Phys. Rev. Lett.* **105** 200402
[47] Zeng K, Yu X, Plenio M B and Wang Z 2024 *Phys. Rev. Lett.* **132** 250801
[48] Souza Alexandre M, Álvarez Gonzalo A and Suter Dieter 2012 *Phil. Trans. R. Soc. A* **370** 4748
[49] Degen C L, Reinhard F and Cappellaro P 2017 *Rev. Mod. Phys.* **89** 035002
[50] Braunstein S and Caves C M 1994 *Phys. Rev. Lett.* **72** 3439
[51] Giovannetti V, Lloyd S and Maccone L 2006 *Phys. Rev. Lett.* **96** 010401
[52] Altarev1 I, Baker C A, Ban G, *et al.* 2009 *Phys. Rev. Lett.* **103** 081602
[53] Zhuang M, Huang J and Lee C 2022 *Quantum* **6** 859
[54] Yen T J, Padilla W J, Fang N, Vier D C, Smith D R, Pendry J B, Basov D N and Zhang X 2004 *Science* **303** 1496
[55] Jensen K, Budvytyte R, Thomas R A, Wang T, Fuchs A M, *et al.* 2016 *Sci. Rep.* **6** 29638
[56] Jiang M, Su H, Garcon A, Peng X and Budker D 2021 *Nat. Phys.* **17** 1402
[57] Sushkov A O 2023 *PRX Quantum* **4** 020101
[58] Zhuang M, Chen S, Huang J and Lee C 2024 *Quantum Front.* **3** 4
[59] Chen S, Zhuang M, Fang R, Chen Y, Han C, Lu B, Huang J and Lee C 2024 *Commun. Phys.* **7** 189
[60] Zhang J, Du P, Jing L, Xu P, You L and Zhang W 2024 *Chin. Phys. B* **33** 030301
[61] Cai J M, Naydenov B, Pfeiffer R, McGuinness L P, Jahnke K D, Jelezko F, Plenio M B and Retzker A 2012 *New J. Phys.* **14** 113023
[62] Morazotti N A C, Silva A H, Audi G, Fanchini F F and Napolitano R J 2024 *Phys. Rev. A* **110** 042601
[63] Trypogeorgos D, Valdés-Curiel A, Lundblad N and Spielma I B 2018 *Phys. Rev. A* **97** 013407
[64] Pham L M, Bar-Gill N, Belthangady C, Sage D L, Cappellaro P, Lukin M D, Yacoby A and Walsworth R L 2012 *Phys. Rev. B* **86** 045214
[65] Shaw A L, Finkelstein R, Tsai R B, Scholl P, Yoon T H, Choi J and Endres M 2024 *Nat. Phys.* **20** 1951
[66] Jiang J, Lu Z, Shen J, Wada T, Kato H and Chen M 2021 *Nat. Commun.* **12** 3843
[67] Aslam N, Zhou H, Urbach E K, Turner M J, Walsworth R L, Lukin M D and Park H 2023 *Nat. Rev. Phys.* **5** 157
[68] Zhou H, Martin L S, Tyler M, Makarova O, Leitao N, Park H and Lukin M D 2023 *Phys. Rev. Lett.* **131** 220803
[69] Jiang J and Chen Q 2024 *Phys. Rev. A* **110** 043714
[70] Butts D L, Kinast J M, Kotru K, Radojevic A M, Timmons B P and Stoner R E 2011 *Phys. Rev. A* **84** 043613
[71] Herbschleb E D, Ohki I, Morita K, Yoshii Y, Kato H, Makino T, Yamasaki S and Mizuochi N 2022 *Phys. Rev. Appl.* **18** 034058